Supporting Information (*SI*) *Appendix* for

Six-rowed spike4 (*Vrs4*) controls spikelet determinacy and row-type in barley

Ravi Koppolu[a,1], Nadia Anwar[b,1], Shun Sakuma[b], Akemi Tagiri[b], Udda Lundqvist[c], Mohammad Pourkheirandish[b], Twan Rutten[d], Christiane Seiler[e], Axel Himmelbach[a], Ruvini Ariyadasa[a], Helmy Mohamad Youssef[a,f], Nils Stein[a], Nese Sreenivasulu[e,g,h], Takao Komatsuda[b] and Thorsten Schnurbusch[a,2]

[a]Department of Genebank, Leibniz-Institute of Plant Genetics and Crop Plant Research (IPK), Gatersleben, D06466, [b]Plant Genome Research Unit, National Institute of Agrobiological Sciences (NIAS), Tsukuba, Japan, 3058602, [c]Nordic Genetic Resource Center, Alnarp, Sweden, SE-23053, [d]Department of Physiology and Cell Biology, Leibniz-Institute of Plant Genetics and Crop Plant Research (IPK), Gatersleben, D06466, [e]Department of Molecular Genetics, Leibniz-Institute of Plant Genetics and Crop Plant Research (IPK), Gatersleben, D06466, [f]Department of Plant Physiology, Faculty of Agriculture, Cairo University, Giza, Egypt, 12613, [g]Research Group Abiotic Stress Genomics, Interdisciplinary Center for Crop Plant Research (IZN), Halle (Saale) D06120, Germany; [h]Grain Quality and Nutrition Center, International Rice Research Institute (IRRI), Metro Manila 1301, Philippines; [1]These authors contributed equally to this work.

Corresponding author: thor@ipk-gatersleben.de

Tel: +49 (0)39482 5-341
Fax: +49 (0)39482 5-595

SI Text

Characterization of deletion in MHOR 318 and MHOR 345.

Because the MHOR 318 and MHOR 345 mutants are *X*-ray induced and are not back-crossed to an isogenic background we characterized the extent of their deletions in the *Vrs4* region using primers derived from the syntenic gene sequences from *Brachypodium*. The synteny in the *Vrs4* region appears to be highly conserved between barley, *Brachypodium* and rice (main text, Fig. 3). The table below shows the list of *Brachypodium* orthologs of barley genes in the *Vrs4* region and their presence or absence in MHOR mutants.

Brachy gene	Annotation	MHOR 318	MHOR 345
Bradi2g04110.1	proactivator polypeptide-like 1-like	Intact	Intact
Bradi2g04117.1	mini-chromosome maintenance complex-binding protein-like	Intact	Intact
Bradi2g04130.1	uncharacterized membrane protein At1g06890-like	Intact	Intact
Bradi2g04140.1	hypothetical protein	Intact	Intact
Bradi2g04150.1	Putative expressed protein	Intact	Intact
Bradi2g04160.1	pentatricopeptide repeat-containing protein At5g66631-like	Intact	Intact
Bradi2g04170.1	Putative expressed protein	Intact	Intact
Bradi2g04180.3	Putative expressed protein	Intact	Intact
Bradi2g04190.1	Putative expressed protein	Intact	Intact
Bradi2g04197.1	zinc finger, C3HC4 type family protein	Deleted	Intact
Bradi2g04210.1	autophagy 18D-like protein	Deleted	Intact
Bradi2g04220.1	DUF246 domain-containing protein At1g04910-like	Deleted	Intact
Bradi2g04230.1	catalytic/ hydrolase	Deleted	Intact
Bradi2g04240.1	flavin-containing monooxygenase YUCCA10-like	*	*
Bradi2g04247.1	flavin-containing monooxygenase YUCCA10-like	*	*
Bradi2g04257.1	flavin-containing monooxygenase YUCCA10-like	*	*
Bradi2g04270.1	ramosa2	Deleted	Deleted
Bradi2g04280.1	RST1	Deleted	Deleted
Bradi2g04290.1	tryptophan aminotransferase-related protein 2-like	Intact	Intact
Bradi2g04297.1	Putative expressed protein	Intact	Intact
Bradi2g04310.1	galactinol--sucrose galactosyltransferase-like	Intact	Intact
Bradi2g04317.1	D111/G-patch domain-containing protein	Intact	Intact
Bradi2g04330.1	probable LRR receptor-like serine/threonine-protein kinase At4g26540-like	Intact	Intact

*Indicates non-syntenic genes in barley. A nucleotide BLAST search against gene rich survey sequences from Morex, Barke and Bowman deposited in IPK barley BLAST server indicated that the orthologous barley genes of *Brachypodium YUCCA10-like* are located somewhere else in the barley genome (Bradi2g04240.1 & Bradi2g04257.1 on chromosomes 2HL and Bradi2g04247.1 on 1H).

Grey highlighted genes are present in the sequenced BAC contig (main text, Fig. 3)

In MHOR 318 the deletion is comparatively larger than in MHOR 345. In both MHOR mutants *HvRA2* and *RESURRECTION1* (*RST1*) were commonly deleted. *RST1* has a putative function in lipid synthesis and embryo development (1).

qRT PCR in *vrs4* mutants BW-NIL(*vrs4.k*), MHOR 318 and MHOR 345.

Expression analysis of *HvRA2* showed lower transcript abundance in BW-NIL(*vrs4.k*) (frame shift mutation) compared to its progenitor MFB104, whereas MHOR 318 and MHOR 345 (deletion

mutants) showed complete absence of *HvRA2* transcripts compared to their progenitors Ackermann's Donaria and Heine's Haisa, respectively (Figure below).

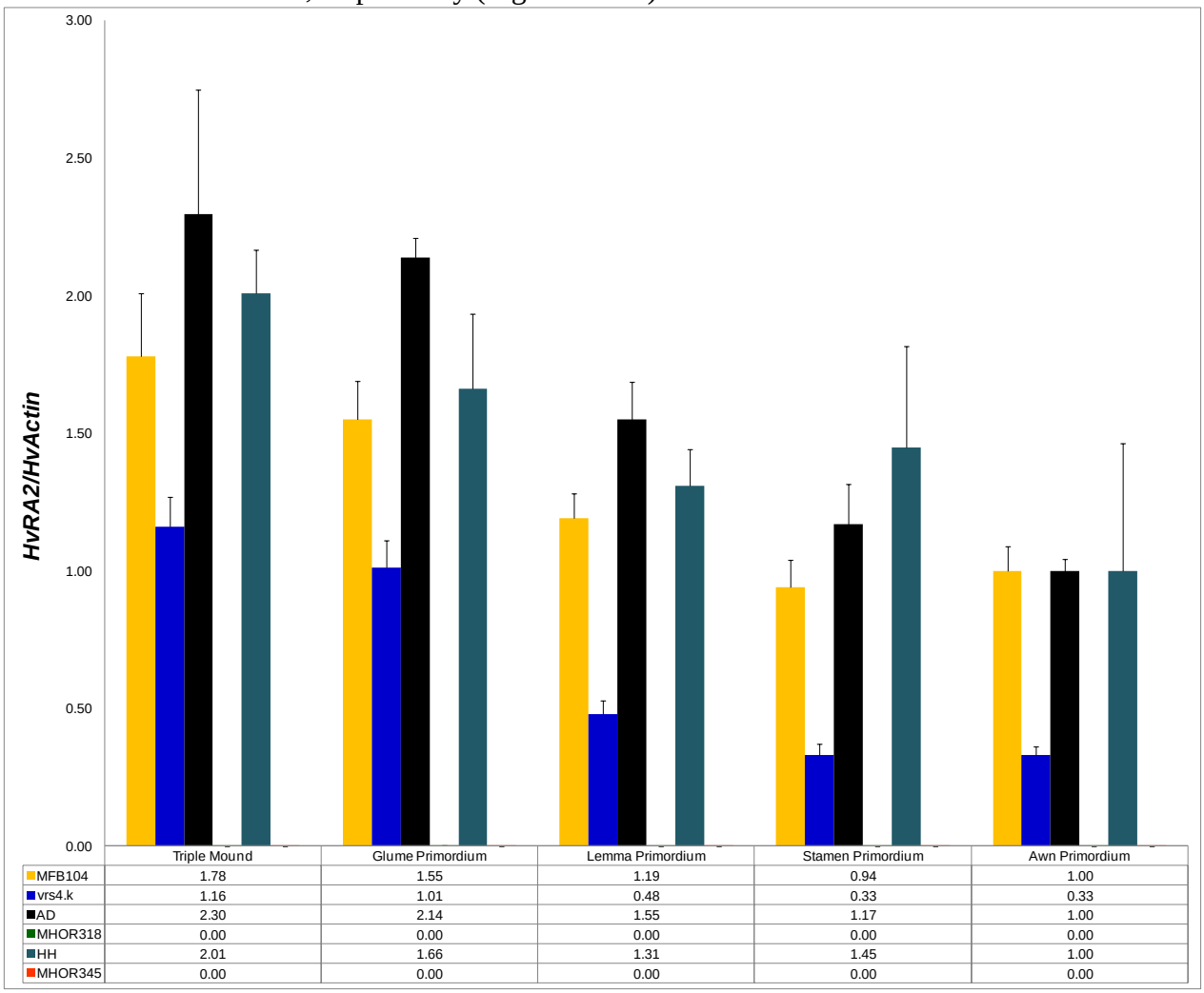

	Triple Mound	Glume Primordium	Lemma Primordium	Stamen Primordium	Awn Primordium
MFB104	1.78	1.55	1.19	0.94	1.00
vrs4.k	1.16	1.01	0.48	0.33	0.33
AD	2.30	2.14	1.55	1.17	1.00
MHOR318	0.00	0.00	0.00	0.00	0.00
HH	2.01	1.66	1.31	1.45	1.00
MHOR345	0.00	0.00	0.00	0.00	0.00

Relative expression of *HvRA2* in BW-NIL(*vrs4.k*), MHOR 318 and MHOR 345 compared to their progenitors. Values in the table below the graph indicate expression of *HvRA2* in wild-types and respective *vrs4* mutants. Error bars indicate mean±S.E. of three replicates.

Allelism test for *int-e.4* and *int-e.20.*

Because the *int-e.4* and *int-e.20* mutant alleles of *vrs4* did not show any molecular lesion within the *HvRA2* ORF the allelism test data is presented below which confirms that these two mutants are in fact allelic to *vrs4* locus. The *int-e.4* and *int-e.20* were crossed to *vrs4.m* and the phenotypes were recorded for F_1 and F_2 stages.

Crossing analyses were done at Svalöv 1989 – 1990.

F_1 : *vrs4.m* × *int-e.4* − *Intermedium* types

F_2: *vrs4.m* × *int-e.4* − 22 *vrs4.m*: 26 *int-e.4*: 61 *Intermedium* types stronger than *int-e.4* but not so pronounced than *vrs4.m*

F_1 : *vrs4.m* × *int-e.20* − *Intermedium* types

F_2: *vrs4.m* × *int-e.20* − 48 *vrs4.m*: 34 *int-e.20*: 68 *Intermedium* types stronger than *int-e.20* but not so pronounced than *vrs4.m*

Additional phenotypic descriptions for *vrs4* mutants.

In wild-type *Vrs4* inflorescence, each spikelet meristem (SM) produces a pair of glumes (inner and outer glumes) (Fig. S1*A*,*D*,*F*). The *vrs4* mutants showed defects in glume development (Fig. S1*C*,*G*) (*SI Dataset* S1*A*), including the occasional absence or rudimentary formation of one or both the glumes and failure in separation of inner and outer glumes (Fig. S2*G*). In some cases the glumes became indeterminate with more than two per spikelet (Fig. S2*F*) and also the glumes were modified to produce additional spikelets/florets (Fig. S2*G*). Additional lemma-like structures with partially or completely developed awns were also observed in both the central (Figure below (*B*), Fig. S1*H*) and lateral spikelets. In case of BW-NIL(*vrs4.k*) and BW-NIL(*mul1.a*) spikelets were pedicelled compared to sessile spikelets of their wild-types (Figure below (*A*)) (2). Another notable phenotype observed in BW-NIL(*vrs4.k*) and BW-NIL(*mul1.a*) was the prostrate growth of tillers compared to erect growth in wild-type Bowman (Figure below (*C*)).

(A) **(B)**

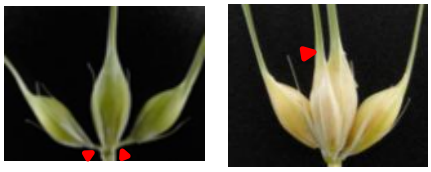

(C)

Differentially regulated genes in microarray analysis.
Based on the 60K microarray analysis in two *vrs4* deletion mutants MHOR 345 (wild-type-Heine's Haisa) and MHOR 318 (wild-type-Ackermann's Donaria) at glume, stamen and awn primordium stages we identified 752 genes that showed robust expression changes with a fold change of >2 at an adjusted *P*-value of <0.05. Among them, 337 genes were down-regulated and 415 genes were up-regulated in the mutants at two or more developmental stages. For the hierarchical clustering analysis shown in *SI Dataset* S1*D*, all 36 arrays were pre-processed and quantile normalized, the co-expression relationships were calculated using Spearman correlation test and complete linkage algorithm implemented in Genespring 12.0. Interestingly, more than 70% of the differentially regulated gene sets are reproduced in the two deletion mutants (*SI Dataset* S1*D* and S1*F*) and the remaining 30% of the changes seen mainly in MHOR 318 could be related to higher extent of deletion beyond *Vrs4*. The genes encoding C3HC4 zinc finger, AUTOPHAGY18D-LIKE in MHOR 318 and RST1 in MHOR 318 and MHOR 345 were highly down-regulated compared to their wild-type counterparts. The down-regulation of these genes is most likely due to the deletion of these genes in the respective MHOR mutants.

SI Materials and Methods

Genetic mapping.
Two F_2 mapping populations were generated by crossing mutant parent *vrs4.k* with two-rowed parents Golden Promise (*vrs4.k* × Golden Promise) and Barke (Barke × *vrs4.k*) at IPK, Germany and another three F_2 mapping populations were generated by crossing two-rowed parent OUH602 (*Hordeum vulgare* ssp. *spontaneum)* with mutant parents *Xc 41.5* (*syn. vrs4.l*) (*Xc 41.5* × OUH602), *int-e.23* (*int-e.23* × OUH602) and *int-e.128* (*int-e.128* × OUH602) at NIAS, Japan. F_2 genotypes of *Xc 41.5* × OUH602 were tested by F_3 analysis (*SI Dataset* S1*H*). For further high resolution mapping, *vrs4.k* × Golden Promise population was utilized. For initial mapping of *vrs4*, 94 to 107 F_2 individuals (Table S1) were analyzed. Segregation between mutant and Wt F_2 plants fitted well with a 3:1 ratio typical for a monogenic recessive trait (Table S1).

The *vrs4* locus was initially reported on chromosome 3H long arm 27.5 cM distal to *uzu* locus (3). The recent genotyping of *vrs4* Bowman introgression lines with BOPA markers showed SNP polymorphisms spanning from 3H short arm until extreme long arm (4). BW-NIL(*int-e.58*) is associated with SNP markers 1_0672 to 2_1083 (positions 38.56 to 156.06 cM), BW-NIL(*mul1.a*) with 1_0762 and 2_0115 (positions 38.56 and 126.83 cM), BW-NIL(*vrs4.k*) with 1_0863 to 1_0926 (positions 64.85 to 85.26 cM) and with 2_1493 to 1_1330 (positions 161.43 to 178.12 cM). In an effort to map *vrs4* to a particular chromosomal region on 3H we developed a VeraCode SNP genotyping assay with 113 BOPA SNPs mapping at regular intervals on 3H. Mapping of 36 and 26 polymorphic markers in *vrs4.k* × Golden Promise and Barke × *vrs4.k* populations localized *vrs4* between markers 3_0571 (32.83cM) and 2_0276 (58.64cM) in Barke × *vrs4.k* and between 3_0953 (40.0cM), 1_1401 (58.01cM) in *vrs4.k* × Golden Promise populations, indicating its presence either on the short arm or close to the centromere. Further marker development in this interval showed strict co-segregation of *vrs4* phenotype with the marker DQ327702 (41.68 cM on the short arm) in all five mapping populations tested (Fig. S4). Linkage analysis of segregation data was carried out using maximum likelihood algorithm of either joinmap 3.0 or MAPMAKER 3.0. Kosambi mapping function was used to convert recombination fractions into map distances. Subsequently 1,086 F_2 individuals were screened to identify recombinant individuals between flanking markers Hv03717

and Hv45740 (*SI Dataset* S1*B*). The 140 recombinant individuals identified were used for further fine mapping of the *vrs4* interval.

DNA preparation.
For DNA preparation, leaf samples at the three leaf stage were collected from all the genotypes (F_2 plants of five mapping populations, fine mapping population from *vrs4.k* × Golden Promise, 20 *vrs4* mutants, respective Wts and 77 diverse barley genotypes used for haplotype analysis). DNA was prepared using either Doyle and Doyle's protocol (5) or the protocol described in Komatsuda et al. 1998 (6).

Haplotype analysis.
Three primer pairs with overlapping fragments (*SI Dataset* S1*C*) covering 2046 bp (987 bp of 5' region, 774 bp ORF and 285 bp 3'UTR) were amplified for direct PCR sequencing using the Sanger method (BigDye Terminator v3.1 Cycle Sequencing Kit; Applied Biosystems). Fluorescently terminated extension products were separated using a capillary-based ABI3730xl sequencing system (Applied Biosystems). Multiple sequence alignments were performed using the ClustalW method (7). Haplotype analysis was conducted using the median joining algorithm implemented in NETWORK 4.6.1.0. A default weight of 10 was applied for all substitutions and indel polymorphisms.

Microarray hybridization and data analysis.
By utilizing 50,000 consensus EST assembly (HarvEST) we synthesized multiple oligos for individual sequences, generated a 244K microarray (Agilent Technologies). A pilot study was conducted to identify and omit oligos with potential for cross hybridization across gene family members from spike meristem tissues. Upon selecting oligos with best Agilent base composition score, a custom eArray was designed to generate 56K Agilent barley microarray (60K × 8 plex format). All unigene sets have been annotated and functionally classified into MapMan functional categories.

Total RNA was isolated from spike meristems collected at glume, stamen and awn primordium stages from two deletion mutants (MHOR 345 and MHOR 318) and respective wild-types (Heine's Haisa and Ackermann's Donaria) using the RNA-queous MircroKit (Invitrogen). RNA concentrations were measured using NanoDrop UV-VIS spectrophotometer (Peqlab) and quality of RNA samples was measured using RNA Nano 6000 kit (Agilent) and Bioanalyzer (Agilent). The Low Input Quick Amp Labeling kit for One-color Microarray-Based Gene Expression Analysis was used for labeling of RNA samples (50ng) using Cyanine3 (Cy3) fluorescent dye following manufacturer's instructions (Agilent). Labeled cRNA samples were subsequently purified using RNeasy mini spin columns (Qiagen) according to the manufacturer's protocol. Quantity of cRNA was measured using NanoDrop, with which specific activity and yield of cRNA were calculated. 600ng of Cy3-labeled, amplified cRNA with a specific activity of above six was used for subsequent hybridization following the steps of the one-color microarray-based gene expression analysis protocol (Agilent). Hybridizations were carried out at 65°C for 17h. Slides were washed and scanned at a high resolution of 2 microns using Agilent DNA Microarray Scanner G2565CA (Agilent). The resultant 36 microarray TIF images were processed to run batch extractions by choosing appropriate grid using Agilent's Feature Extraction Software version 11.0. The quantified feature text file is first analysed for quality checks using Agilent QC chart tool. The qualified experiments were further processed, at first raw data (gene expression) was quantile normalized and fold changes were calculated between mutant and wild-type samples for all developmental stages. The differentially regulated gene sets

(>2.0 folds), with multiple correction using Bonferroni method (P<0.05) were identified. Top regulated genes were subjected to the co-expression analysis using spearman correlation test and complete linkage algorithm implemented in Genespring 12.0. Only differentially regulated genes in common between both mutants (MHOR 318 and MHOR 345) were considered for further analysis and interpretation.

SI Figures

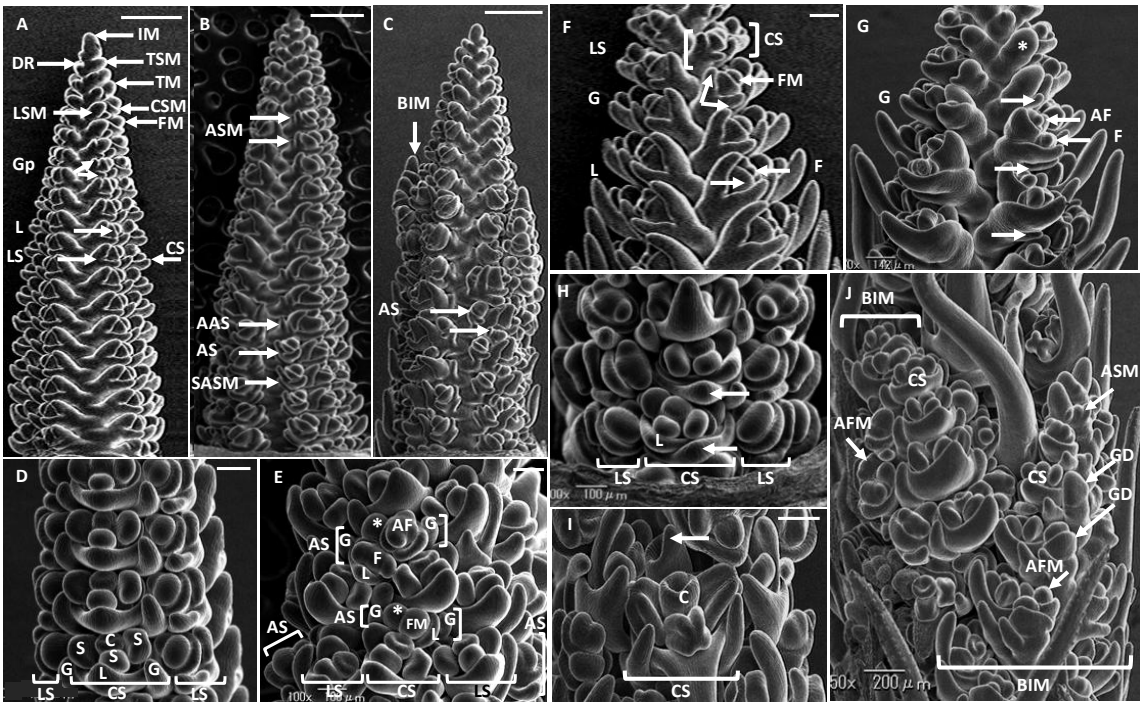

Fig. S1. SEM analysis of wild-type (Piroline) and *vrs4* mutant (*vrs4.l*) spikes.
(*A*-*C*) Lateral view of inflorescences at awn primordium stage (*A*) Wt inflorescence shows triple spikelet meristem (TSM) producing one central spikelet meristem (CSM) and two lateral spikelet meristems (LSMs), leading to central spikelet (CS) and lateral spikelets (LSs). Gp, glume primordium of LS (*B*) *vrs4* inflorescence (Autumn-sown) showing LSs at an advanced stage of development, and additional spikelet meristems (ASMs) which either remain rudimentary as aborted additional spikelets (AASs) or form additional spikelets (ASs). SASM, Secondary additional spikelet meristem. (*C*) *vrs4* inflorescence (Spring-sown) showing branch-like inflorescence meristem (BIM), ASs, and glume defects (upper half). (*D*) Wt inflorescence showing two LSs and a CS having two glumes (G), and one floret containing one lemma (abaxial), three stamens (S) and one carpel. (*E*) *vrs4* inflorescence showing advance staged LSs, and ASs with LSs and CSs. ASs show glumes, lemma (abaxial) and a floral meristem (FM) (bottom), or a floret (top) having an additional floret (AF) on its rachilla. Asterisk indicates further development on rachilla of FM or AF. (*F*) Wt inflorescence showing LSs containing a single FM or floret with lemma (abaxial) and a pair of glumes. (*G*) *vrs4* inflorescence showing AF on rachilla of floret in opposite orientation. LSs having no glumes (asterisk) or a single glume (right-headed arrows) are visible. (*H*) *vrs4* inflorescence showing an additional lemma-like structure (arrows) with the lemma in CSs. (*I*) *vrs4* inflorescence showing an additional carpel (arrow) in opposite orientation to carpel in CS. (*J*) *vrs4* inflorescence showing two

BIMs having ASMs, AFMs and glume defects (GD). Scale bars: 500μm in a-c; 100μm in d-e, h; 142μm in f-g, i; 200μm in j.

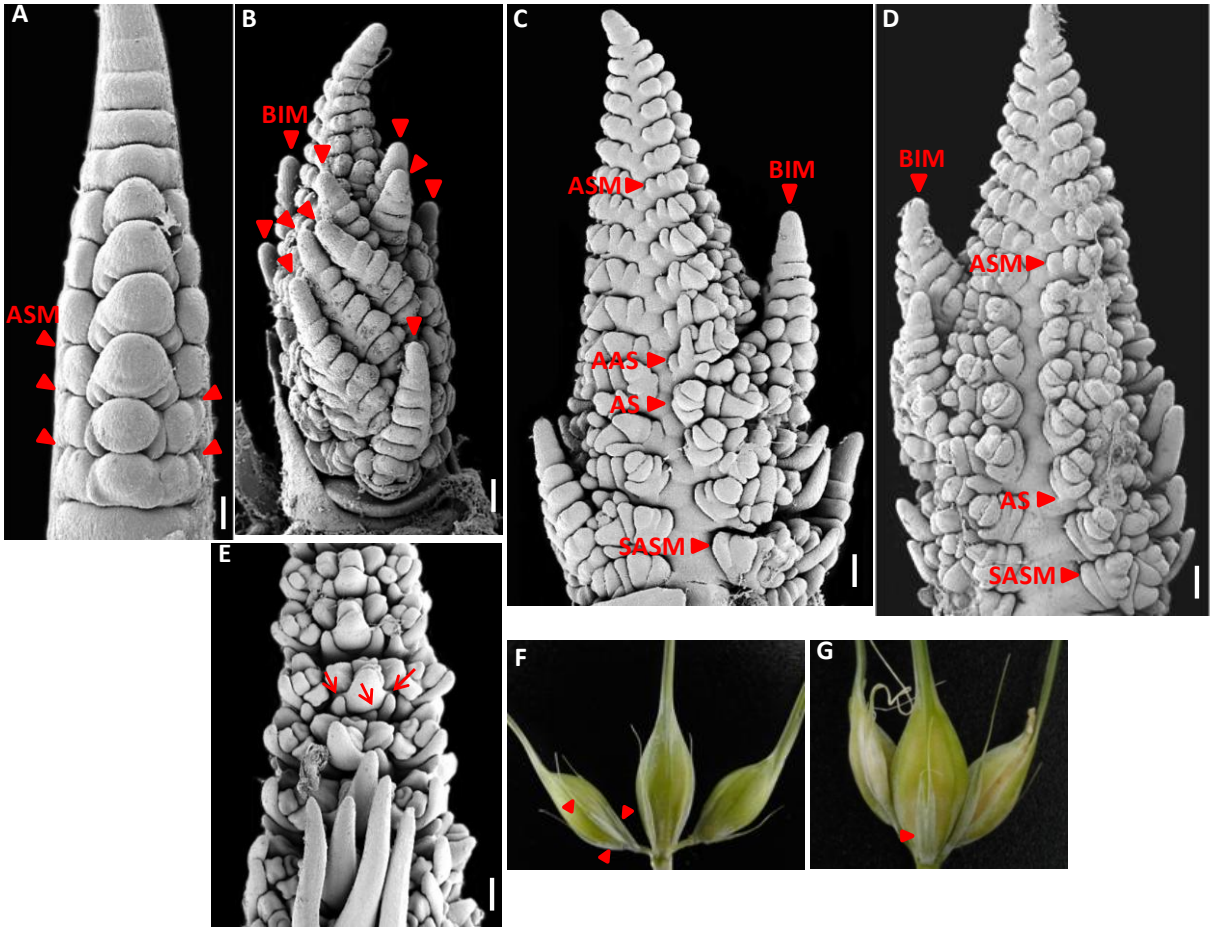

Fig. S2. SEM analysis of BW-NIL(*mul1.a*) and BW-NIL(*vrs4.k*).
(*A*) BW-NIL(*mul1.a*) mutant inflorescence at lemma primordium stage, showing initiation of additional spikelet meristem (ASMs) indicated by red triangles, on each side of the triple mound. (*B*) BW-NIL(*vrs4.k*) mutant inflorescence showing high proliferation of branch-like inflorescence meristems (BIMs) indicated by red triangles at stamen primordium stage. (*C-D*) BW-NIL(*vrs4.k*) (*C*) and BW-NIL(*mul1.a*) (*D*) mutant inflorescences showing ASMs, additional spikelets (ASs), aborted additional spikelets (AASs), secondary additional spikelet meristems (SASM), and branch-like inflorescence meristems (BIM) at awn primordium stage. (*E,F*) Pictures show loss of determinacy in glume development resulting in more than two glumes per spikelet. Three glumes per spikelet are seen at awn primordium stage (*E*) and at maturity (*F*). (*G*) Spikelet showing partially differentiated inner and outer glumes at maturity. Scale bars: 400μm in *A* and 700μm in *B-E*.

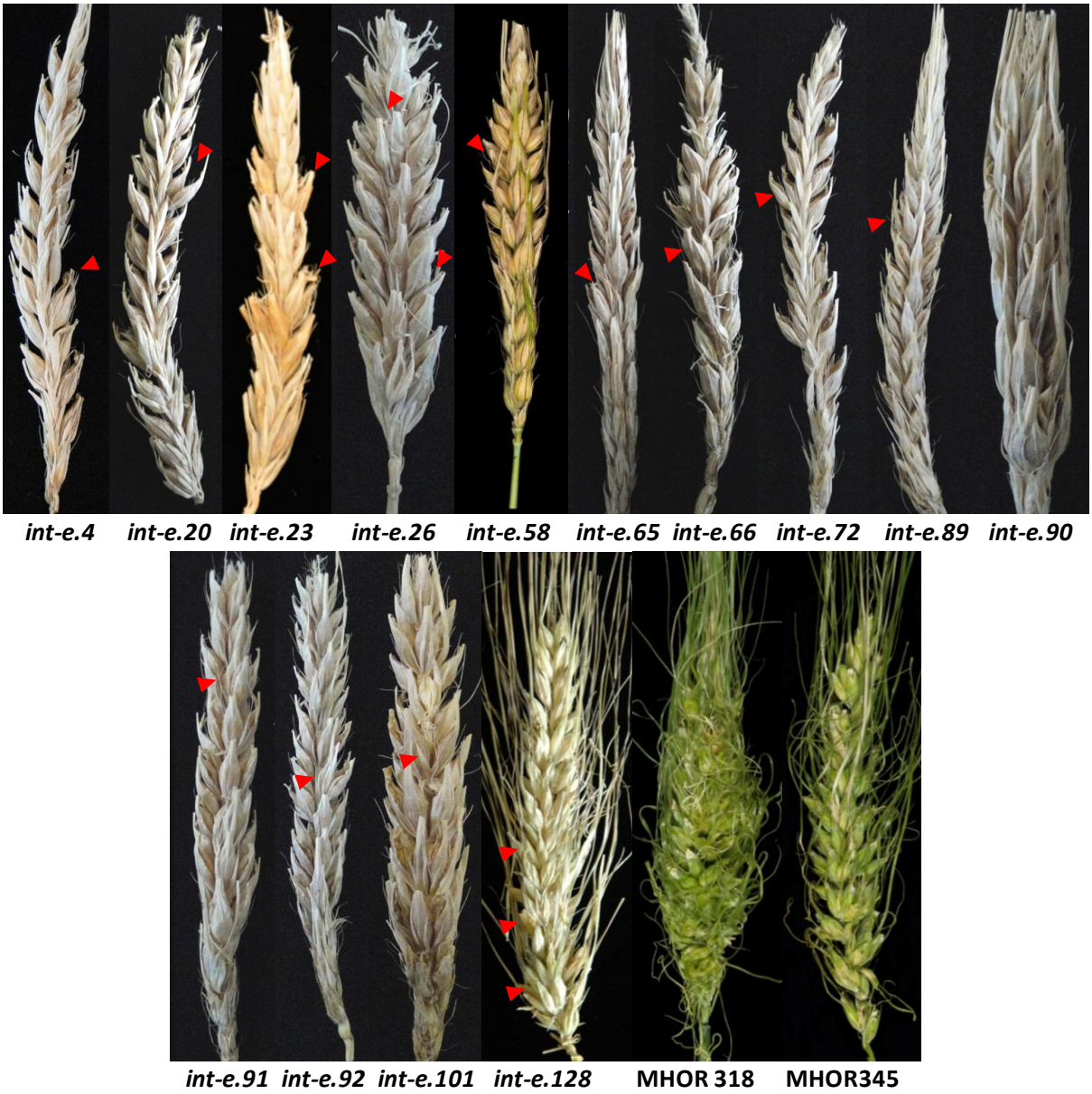

Fig. S3. Different *vrs4* mutant alleles showing loss of spikelet determinacy (Red triangles mark the presence of additional spikelets due to the indeterminate nature of the TSM). The MHOR mutants MHOR 318 and MHOR 345 show a high degree of indeterminacy of the TSM probably due to the complete deletion of *HvRA2*.

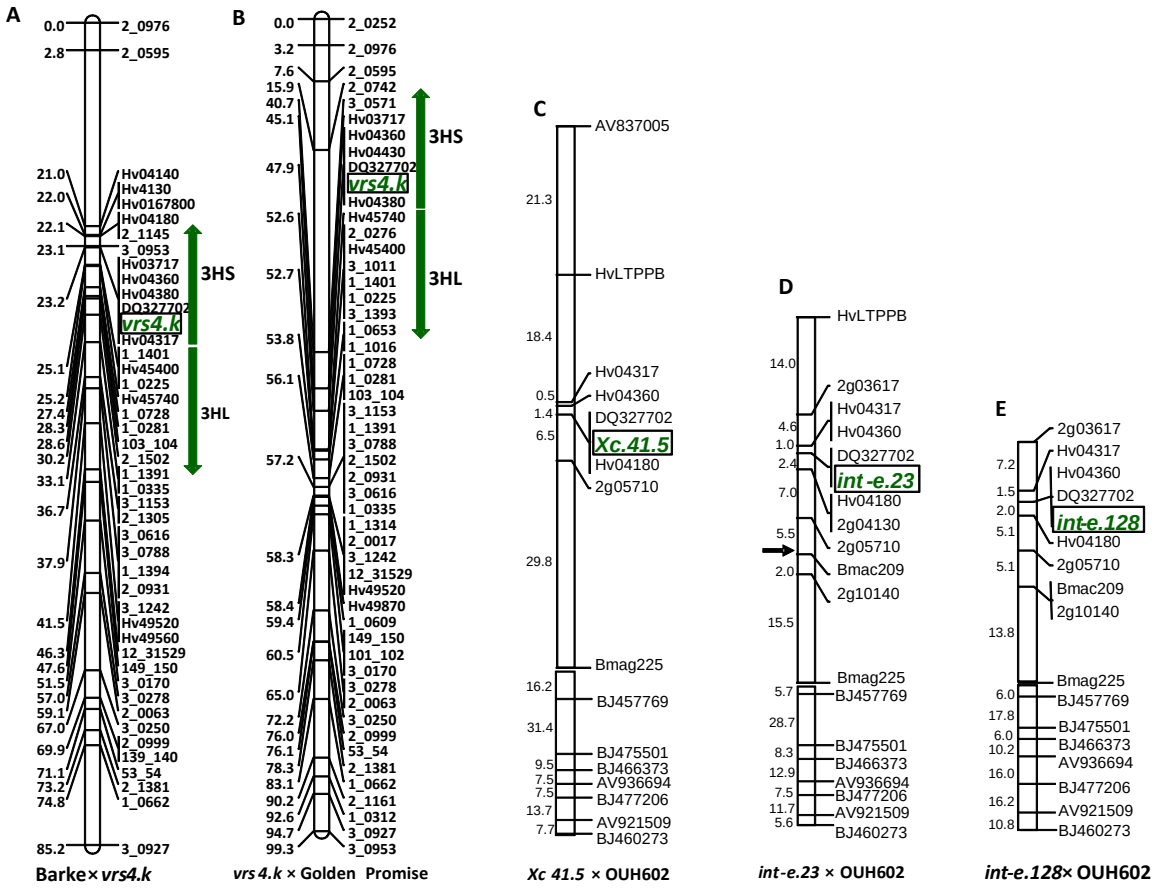

Fig. S4. Linkage maps for the *vrs4* locus on barley chromosome 3H.
(*A*-*E*) Linkage maps were developed based on five F_2 mapping populations. The scale of the maps has been reduced in the lower parts for *C*,*D*,*E*. The number of gametes analyzed in the upper parts (above Bmag225) are 214 (*C*), 210 (*D*) and 214 (*E*). 58 gametes were analyzed in the lower parts (below Bmag225) for *C*,*D*,*E*. Map distances are shown in centiMorgans. Arrow shows the location of centromere. *Xc 41.5 syn. vrs4.l.*

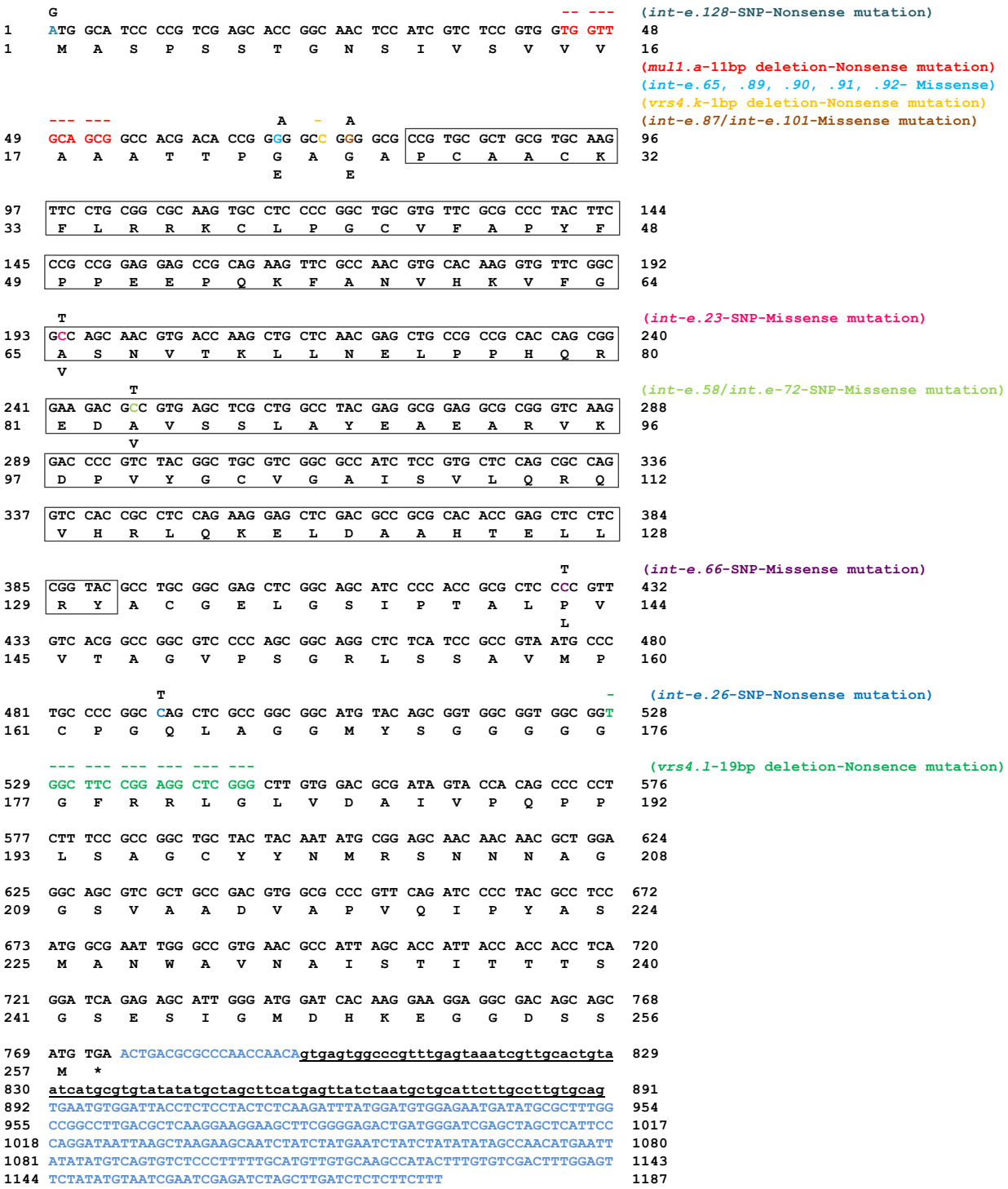

Fig. S5. *HvRA2* (*Vrs4*) nucleotide and protein sequences showing mutated positions and effects for sixteen *Vrs4* mutant alleles. Small deletions and SNPs in the *vrs4* mutant alleles leading to frame shifts, non-synonymous changes and premature stop codons have been indicated in respective colors with that of mutant alleles. The sequence in the boxed area represents the LOB domain. The blue highlighted sequence at the 3' end marks the 3'-UTR, the underlined region within the 3'-UTR indicates the intron.

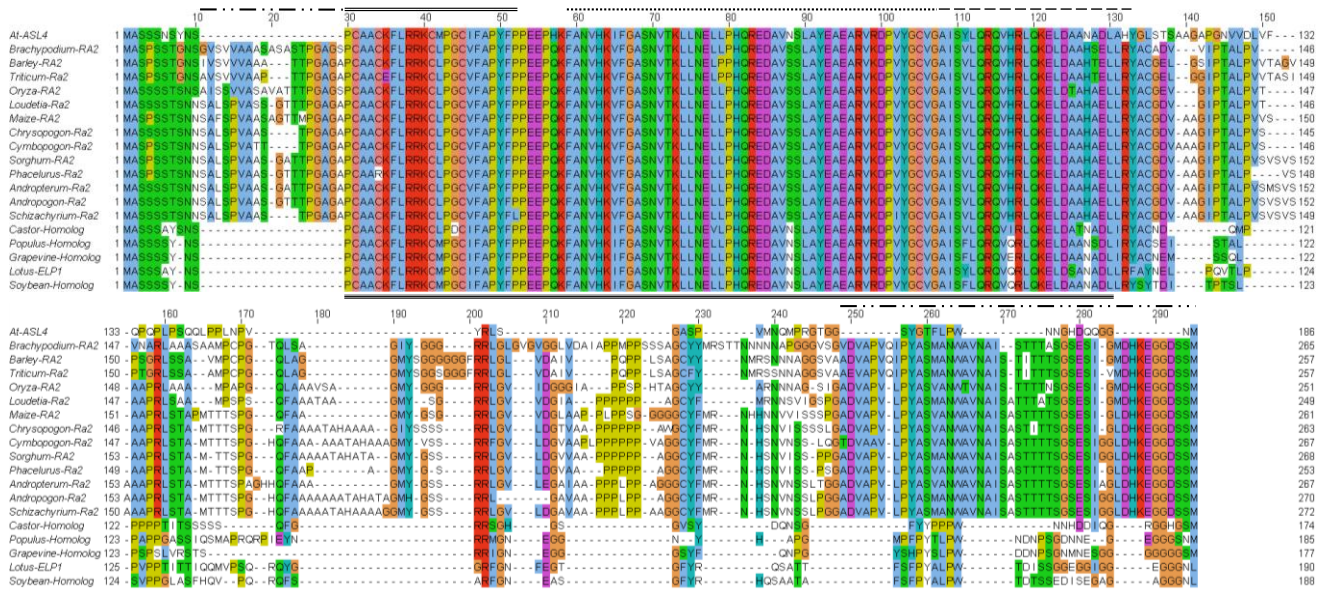

Fig. S6. RA2 and RA2-like proteins in grasses and eudicots.
Multiple sequence alignment of RA2 proteins in monocotyledonous and dicotyledonous species. The unique grass specific domains at N-terminal and C-terminal are indicated with a combination of dashed and dotted lines; LOB domain is marked with a triple line (The components of LOB domain such as Cysteine rich region, GAS block and Leucine Zipper coiled coil motif are marked with double, dotted and dashed lines respectively. GenBank accession numbers for RA2 & RA2-like proteins are listed in Table S6.

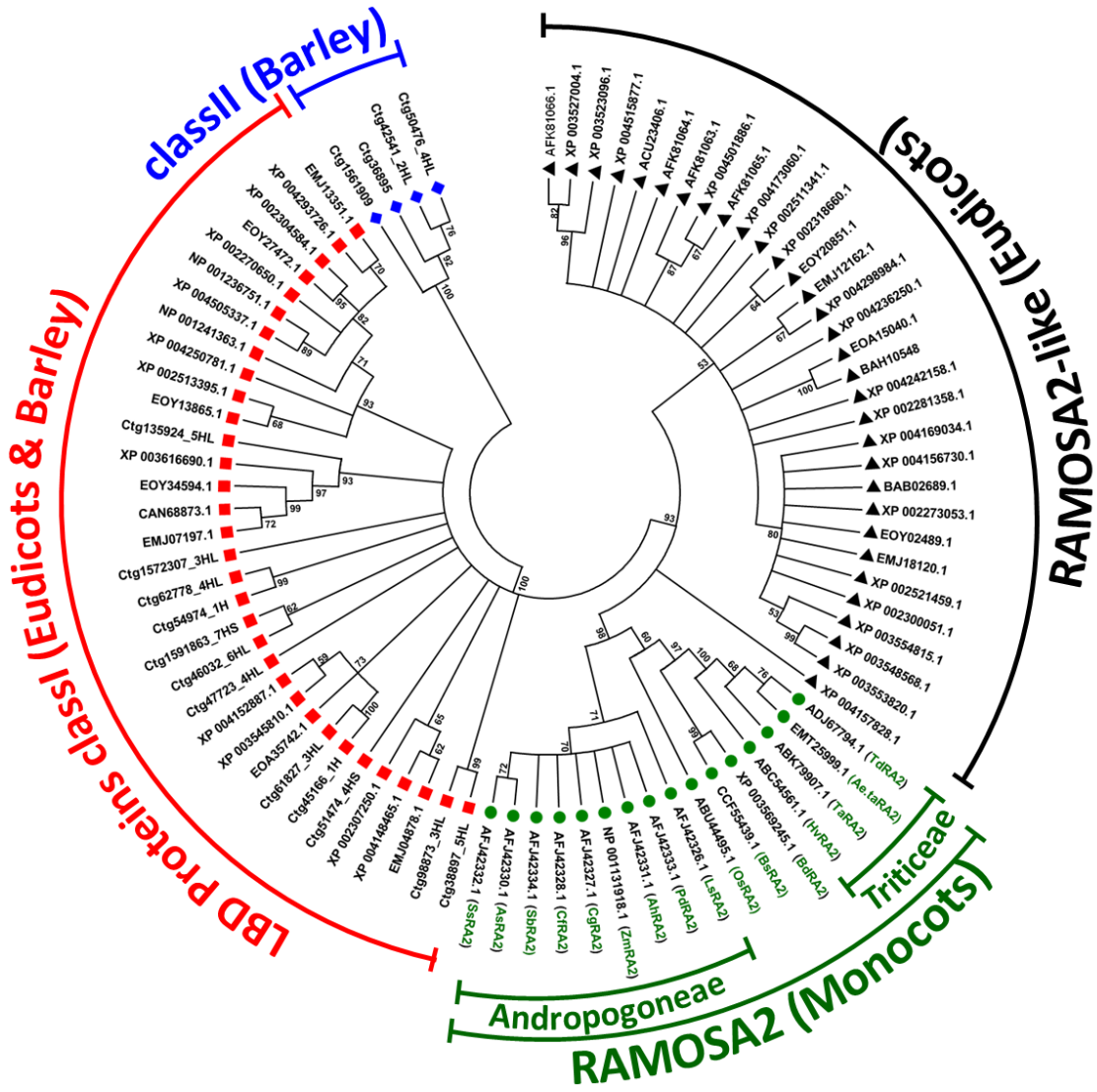

Fig. S7. Phylogenetic analysis of RAMOSA2 orthologs/homologs and other LBD proteins.
A maximum likelihood phylogenetic tree (condensed tree) of RAMOSA2 orthologs (RAMOSA2 proteins from grasses) and homologs (RA2-LIKE proteins from eudicot species) together with other LBD proteins from barley and eudicots. From the phylogenetic tree two separate clades are evident; one clade carrying the LBD proteins other than RAMOSA2 orthologs/homologs and the other with RAMOSA2 orthologs and homologs. The clade carrying RAMOSA2 orthologs/homologs has two sub clades, one with the RAMOSA2 orthologs from grasses and the other with RAMOSA2 homologs. Eudicot homologs of RAMOSA2 are indicated by black triangles, orthologs from monocots are indicated by green circles, class I barley and Eudicot LBD proteins other than RAMOSA2 orthologs/homologs are marked by red squares. Class II barley LBD proteins indicated by blue squares are clearly separated from all the remaining class I LOB domain proteins. For descriptions of class I and class II LOB domain proteins refer to Shuai et al. 2002 (8). Td: *Triticum durum*; Ae.ta: *Aegilops tauschi*; Ta: *Triticum aestivum*; Hv: *Hordeum vulgare*; Bd: *Brachypodium distachyon*; Bs: *Brachypodium sylvaticum*; Os: *Oryza sativa*; Ls: *Loudetia spp.*; Pd: *Phacelurus digitatus*; Ah: *Andropogon hallii*; Zm: *Zea mays*; Cg: *Chrysopogon gryllus*; Cf: *Cymbopogon*

flexosus; Sb: *Sorghum bicolor*; As: *Andropterum stolzii*; Ss: *Schizachyrium sanguineum*. (Please refer to Table S6 for the details of protein accessions used in phylogenetic analysis).

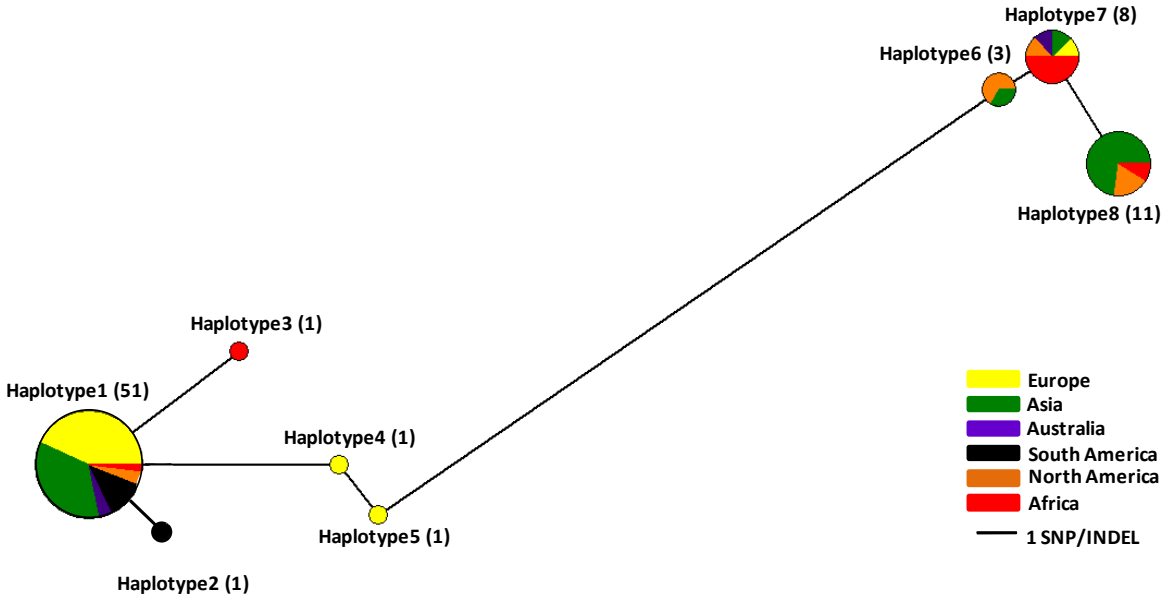

Fig. S8. *HvRA2* nucleotide-haplotype analysis.
Circles denote the relative number of samples represented in each *Vrs4* haplotype. Number of accessions within a particular haplotype is indicated in brackets. Pie slices within the circles indicate geographic distribution of haplotypes. Lines connecting haplotypes denote number of mutations (SNPs or deletions) that distinguish different haplotypes. (See *SI Dataset* S1*C* for haplotype structure of the eight haplotypes identified).

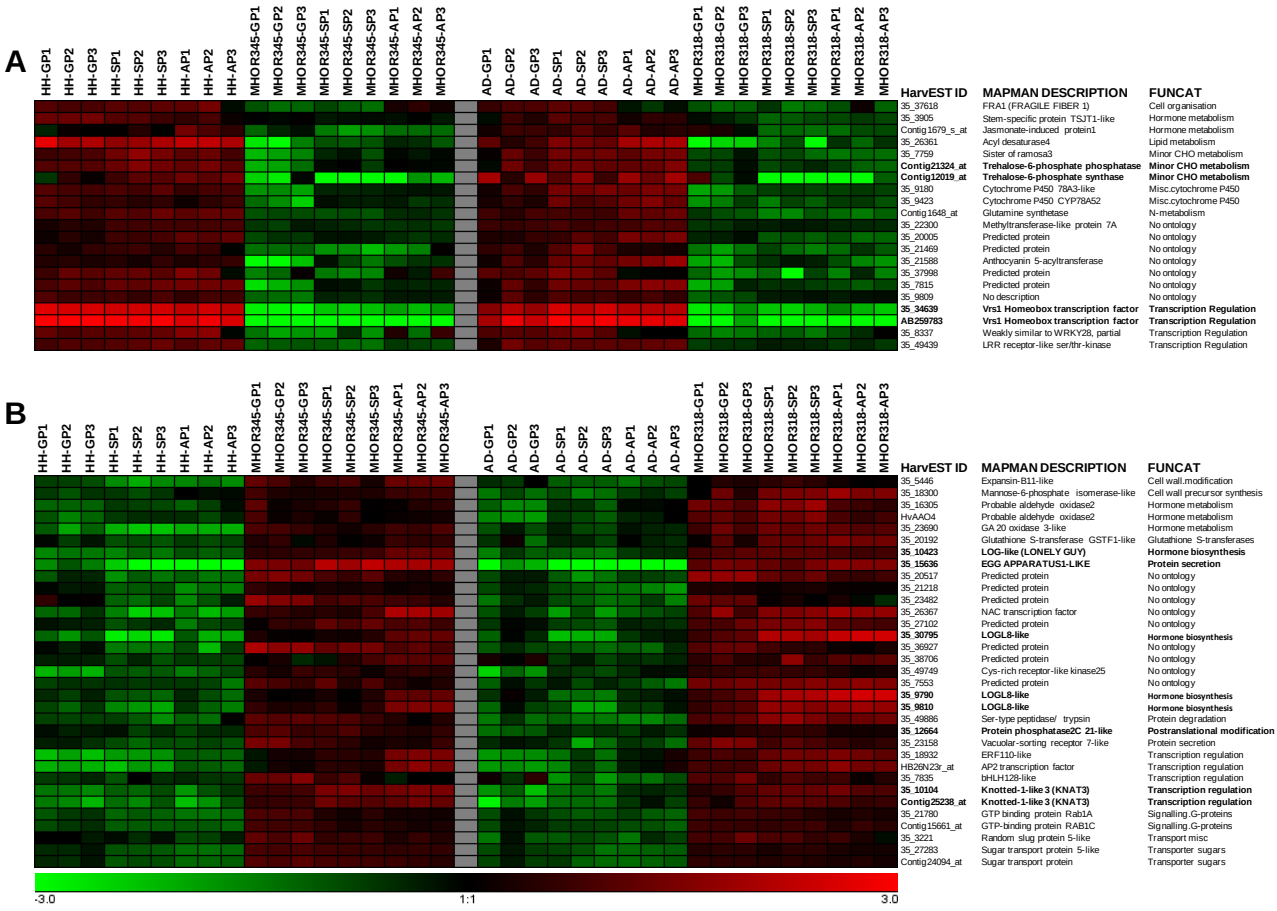

Fig. S9. Transcriptome analysis of *vrs4* using microarray.
(*A*-*B*) Microarray heat maps show genes conjointly down-regulated (*A*), up-regulated (*B*) in two *vrs4* deletion mutants (MHOR 318 and MHOR 345) and their respective wild-types (Ackermann's Donaria and Heine's Haisa). GP: glume primordium, SP: stamen primordium, AP: awn primordium. The scale at the bottom of the heat maps indicates the level of differential regulation observed for different genes between Wt and mutant (green color indicates down-regulation and red color indicates up-regulation).

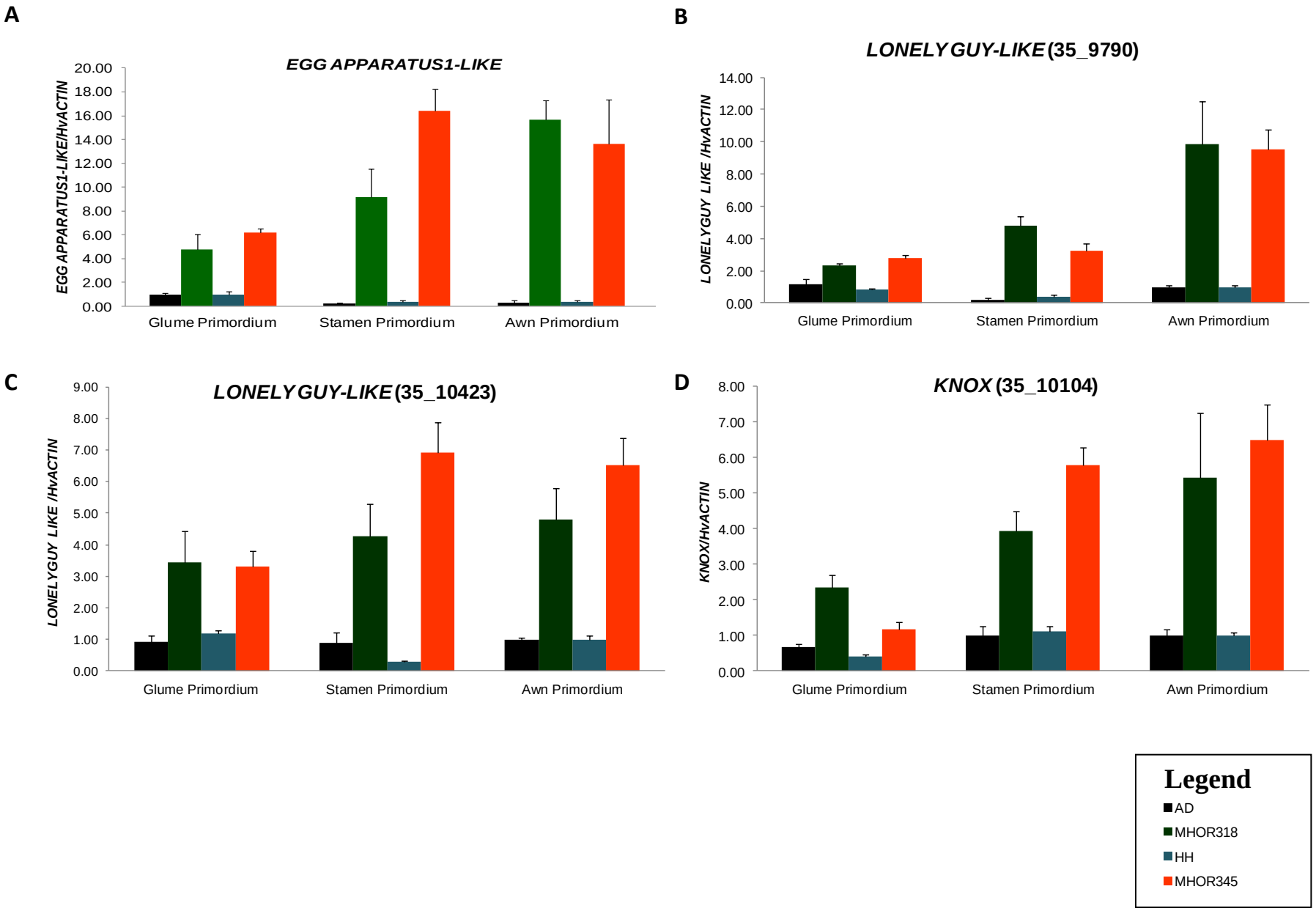
A
EGG APPARATUS1-LIKE
EGG APPARATUS1-LIKE/HvACTIN
20.00
18.00
16.00
14.00
12.00
10.00
8.00
6.00
4.00
2.00
0.00
Glume Primordium
Stamen Primordium
Awn Primordium
B
LONELY GUY-LIKE (35_9790)
LONELYGUY LIKE /HvACTIN
14.00
12.00
10.00
8.00
6.00
4.00
2.00
0.00
Glume Primordium
Stamen Primordium
Awn Primordium
C
LONELY GUY-LIKE (35_10423)
LONELYGUY LIKE /HvACTIN
9.00
8.00
7.00
6.00
5.00
4.00
3.00
2.00
1.00
0.00
Glume Primordium
Stamen Primordium
Awn Primordium
D
KNOX (35_10104)
KNOX/HvACTIN
8.00
7.00
6.00
5.00
4.00
3.00
2.00
1.00
0.00
Glume Primordium
Stamen Primordium
Awn Primordium
Legend
AD
MHOR318
HH
MHOR345

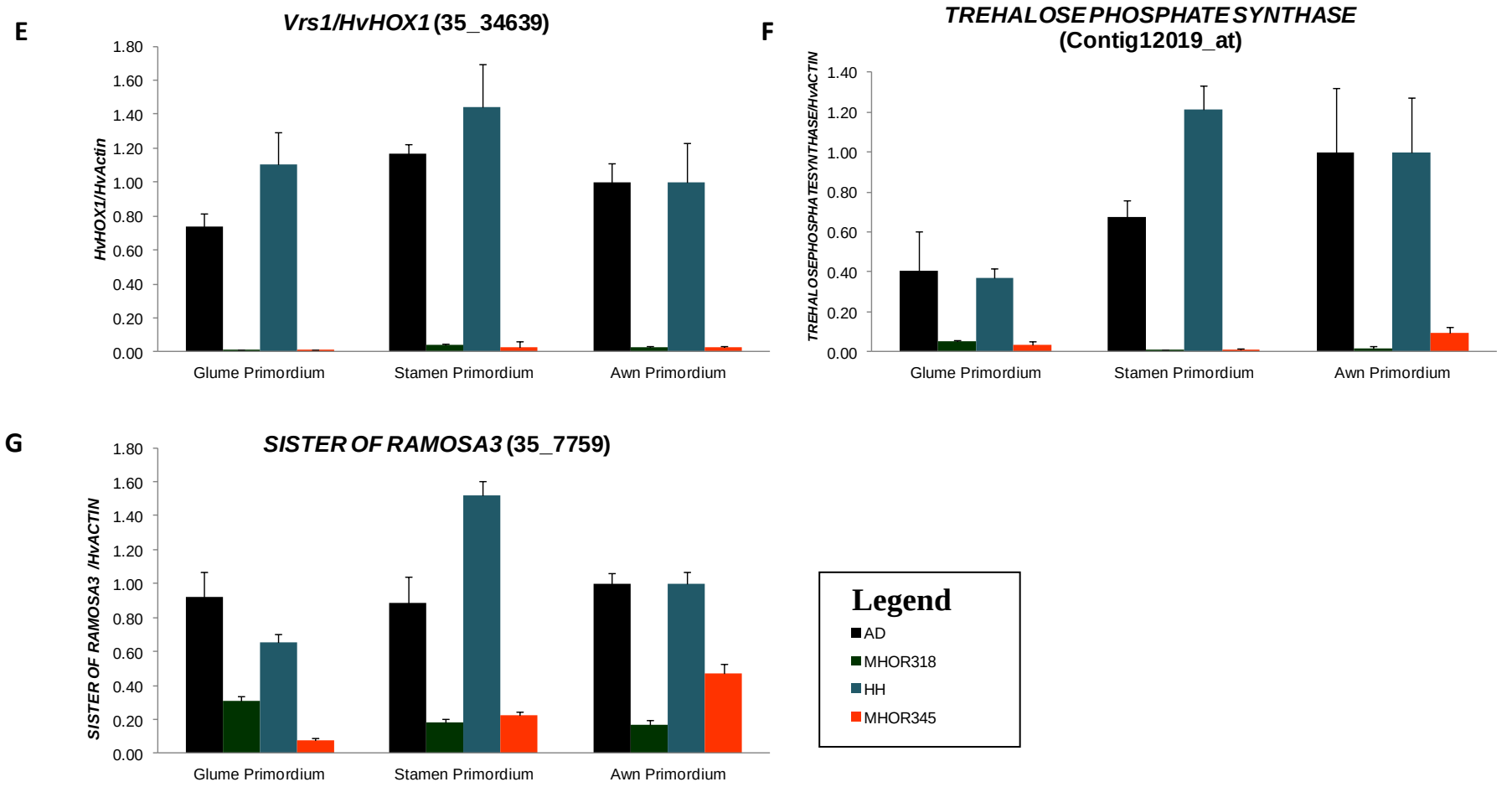

Fig. S10. qRT-PCR validation of differentially regulated genes identified in the *vrs4* microarray experiment. (*A-D*) qRT-PCR validation of genes up-regulated in MHOR 318, MHOR 345 in comparison to their respective wild-types Ackermann's Donaria (AD) and Heine's Haisa (HH). The validated genes include *EGG APPARTUS1* (*A*), *LONELY GUY-LIKE* (*B-C*) and *KNOX* (*D*). (*E-G*) qRT-PCR validation of genes down-regulated in mutants in comparison to their respective wild-types, include *Vrs1* (*E*) *TREHALOSE PHOSPHATE SYNTHASE* (*F*), *SISTER OF RAMOSA3* **(***G*). RNA samples from three spike developmental stages (glume primordium, stamen primordium and awn primordium) were analyzed. Mean ± S.E of three biological replicates is shown.

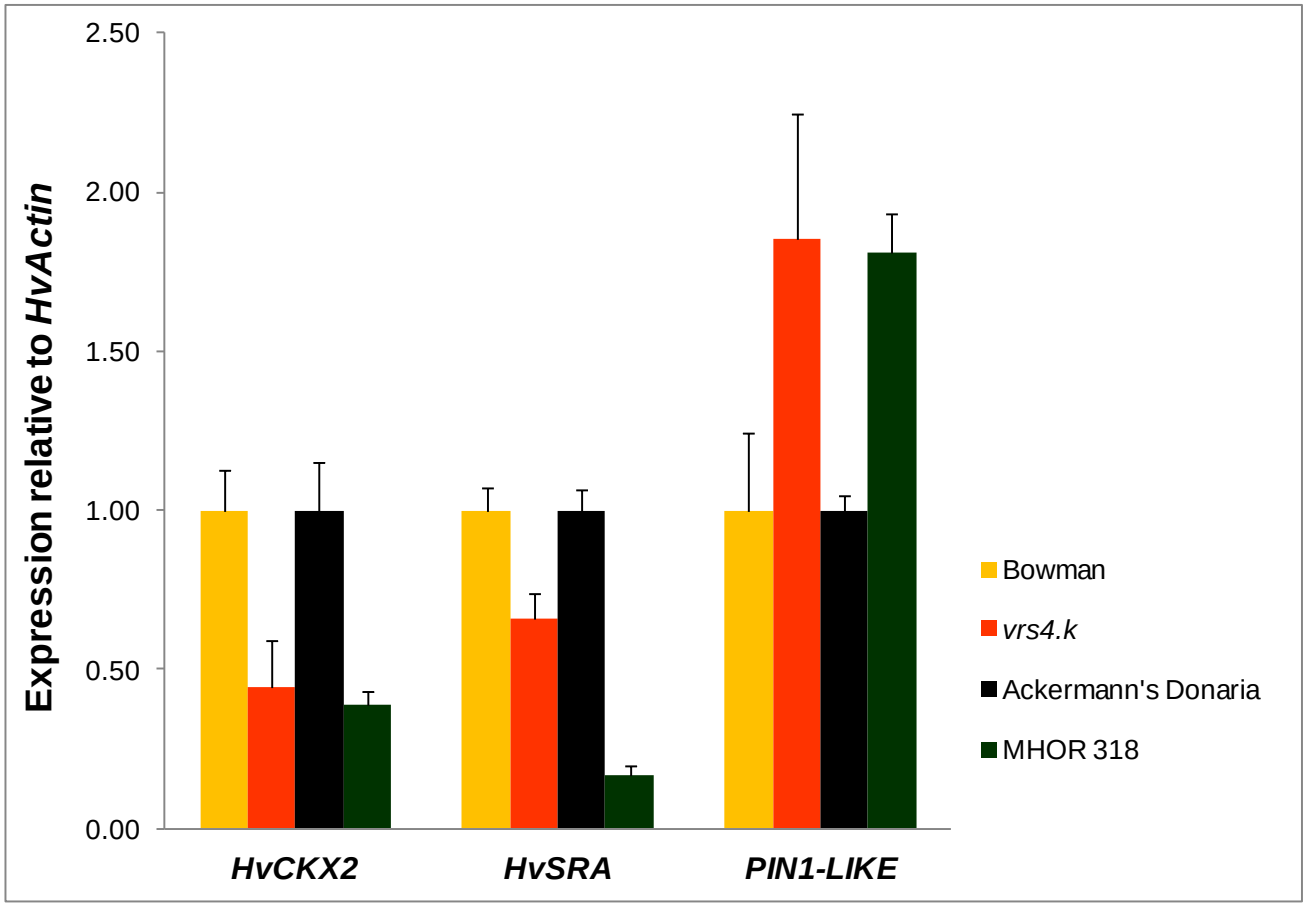

Fig. S11. Relative expression of *HvCKX2*, *HvSRA* and *HvPIN1-LIKE* in BW-NIL(*vrs4.k*), MHOR 318 and their respective wild-types Bowman and Ackermann's Donaria. RNAs sampled at awn primordium were used to quantify the expression. Constitutively expressed *HvActin* gene was used to normalize expression of target genes. Error bars indicate mean±S.E. of three replicates.

SI Tables

Table S1. Segregation analysis of *vrs4* mutants in five F_2 mapping populations.

Crosses	**# of F_2 individuals (gametes)**	**Wild-type**	**Mutant**	**χ2/P-value for 3:1**
Xc 41.5 × OUH602	107 (214)	84	23	0.701/0.402
int-e.23 × OUH602	105 (210)	84	21	1.400/0.236
int-e.128 × OUH602	107 (214)	88	19	2.994/0.083
vrs4.k × Golden Promise	94 (188)	71	23	0.014/0.905
Barke × *vrs4.k*	94 (188)	71	23	0.014/0.905

Table S2. Annotations of putative genes present in the *vrs4* syntenic interval of *Brachypodium* based on initial mapping.

***Brachypodium* gene**	**Annotation**	**e-value**
Bradi2g03717.1	peptidase M48 like	0.0
Bradi2g03730.1	pentatricopeptide repeat-containing protein	0.0
Bradi2g03740.1	sphingosine-1-phosphate lyase-like	0.0
Bradi2g03750.1	Putative expressed protein	0.0
Bradi2g03760.1	40S ribosomal protein S5-2-like	7E-149
Bradi2g03770.1	Putative expressed protein	0.0
Bradi2g03777.1	monocopper oxidase-like protein SKU5-like isoform 1	0.0
Bradi2g03790.1	BFR2-like	0.0
Bradi2g03800.1	cysteine synthase, chloroplastic/chromoplastic-like isoform 1	0.0
Bradi2g03807.1	GDSL esterase/lipase	0.0
Bradi2g03820.1	FKBP12-interacting protein of 37 kDa-like	0.0
Bradi2g03825.1	embryonic abundant protein 1-like	4E-46
Bradi2g03830.1	transcription factor bHLH51-like	2E-154
Bradi2g03840.1	pyruvate decarboxylase isozyme 2-like	0.0
Bradi2g03850.1	wall-associated receptor kinase 2-like	0.0
Bradi2g03860.1	E3 ubiquitin-protein ligase SIAH1-like	4E-116
Bradi2g03870.1	E3 ubiquitin-protein ligase SIAH1-like	7E-77
Bradi2g03880.1	receptor-like protein 12-like	2E-170
Bradi2g03890.1	receptor-like protein 12-like	0.0
Bradi2g03900.1	receptor-like protein 12-like	2E-165
Bradi2g03910.1	receptor-like protein 12-like	0.0
Bradi2g03920.1	LRR receptor-like serine/threonine-protein kinase GSO1-like	0.0
Bradi2g03930.1	Putative expressed protein	2E-52
Bradi2g03940.5	Putative expressed protein	0.0
Bradi2g03947.1	DEAD-box ATP-dependent RNA helicase	0.0
Bradi2g03960.1	DEAD-box ATP-dependent RNA helicase 18-like	0.0
Bradi2g03970.1	probable protein phosphatase 2C 1-like	7E-177
Bradi2g03980.1	Golgi to ER traffic protein 4 homolog	0.0
Bradi2g03990.1	breast cancer 2 -like	0.0
Bradi2g04000.1	dehydration-responsive element-binding protein 2A-like	0.0
Bradi2g04010.1	E3 ubiquitin-protein ligase RING1-like	0.0
Bradi2g04020.1	zinc transporter 1-like	6E-113
Bradi2g04030.1	uncharacterized protein	0.0
Bradi2g04040.3	KEAP1	2E-163
Bradi2g04050.1	Putative expressed protein	0.0
Bradi2g04060.1	Putative expressed protein	0.0
Bradi2g04070.1	Putative expressed protein	0.0
Bradi2g04080.1	Putative expressed protein	0.0

Bradi2g04090.1	Putative expressed protein	0.0
Bradi2g04100.1	probable ubiquitin-conjugating enzyme E2 25-like	1E-154
Bradi2g04110.1	proactivator polypeptide-like 1-like	1E-163
Bradi2g04117.1	mini-chromosome maintenance complex-binding protein-like	0.0
Bradi2g04130.1	uncharacterized membrane protein At1g06890-like	0.0
Bradi2g04140.1	hypothetical protein	0.0
Bradi2g04150.1	Putative expressed protein	0.0
Bradi2g04160.1	pentatricopeptide repeat-containing protein At5g66631-like	0.0
Bradi2g04170.1	Putative expressed protein	0.0
Bradi2g04180.3	Putative expressed protein	0.0
Bradi2g04190.1	Putative expressed protein	0.0
Bradi2g04197.1	zinc finger, C3HC4 type family protein	0.0
Bradi2g04210.1	autophagy 18D-like protein	0.0
Bradi2g04220.1	DUF246 domain-containing protein At1g04910-like	0.0
Bradi2g04230.1	catalytic/ hydrolase	6E-125
Bradi2g04240.1	flavin-containing monooxygenase YUCCA10-like	3E-128
Bradi2g04247.1	flavin-containing monooxygenase YUCCA10-like	0.0
Bradi2g04257.1	flavin-containing monooxygenase YUCCA10-like	0.0
Bradi2g04270.1	ramosa2	3E-91
Bradi2g04280.1	RST1	0.0
Bradi2g04290.1	tryptophan aminotransferase-related protein 2-like	0.0
Bradi2g04297.1	Putative expressed protein	0.0
Bradi2g04310.1	galactinol--sucrose galactosyltransferase-like	0.0
Bradi2g04317.1	D111/G-patch domain-containing protein	1E-88
Bradi2g04330.1	probable LRR receptor-like serine/threonine-protein kinase At4g26540-like	0.0
Bradi2g04340.1	Putative expressed protein	0.0
Bradi2g04350.1	F-box domain containing protein	8E-98
Bradi2g04360.1	putative ZmEBE-1 protein	0.0
Bradi2g04370.1	Putative expressed protein	0.0
Bradi2g04380.1	universal stress protein A-like protein-like	1E-117

Table S3. List of barley LOB domain (LBD) containing genes used for phylogenetic analysis.

LBD gene contig	LBD Class	Partial/Complete
Ctg2547112_3HS	Class I	Complete
Ctg45166_1H	Class I	Complete
Ctg51474_4HS	Class I	Complete
Ctg135924_5HL	Class I	Complete
Ctg54974_1H	Class I	Complete
Ctg46032_6HL	Class I	Complete
Ctg1572307_3HL	Class I	Complete
Ctg62778_4HL	Class I	Complete
Ctg47723_4HL	Class I	Complete
Ctg1591863_7HS	Class I	Complete
Ctg38897_5HL	Class I	Complete
Ctg61827_3HL	Class I	Complete
Ctg98873_3HL	Class I	Complete
Ctg42541_2HL	Class II	Complete
Ctg50476_4HL	Class II	Complete
Ctg1561909	Class II	Complete
Ctg36895	Class II	Complete
Ctg39781_4HL	Class I	Partial
Ctg63283_3HL	Class I	Partial
Ctg1559770_4HL	Class I	Partial
Ctg39524_1H	Class I	Partial
Ctg41408_4HS	Class I	Partial
Ctg40527_1H	Class I	Partial

Contig IDs represent LBD gene containing Morex contigs available from IPK Barley BLAST server

Table S4. *vrs4* mutant descriptions.

#	Mutant allele	Progenitor	Background/ corresponding *Vrs1* allele	Mutagen	Mapping study	Type of mutation	Polymorphism/Position*
1	*int-e.4*	Bonus	Bonus/*Vrs1.b3* (9)**	Neutrons	Lundqvist 1991(10)	No mutation	—
2	*int-e.20*	Foma	Foma/*Vrs1.b3* (9)	Neutrons	Lundqvist 1991(10)	No mutation	—
3	*int-e.23*	Foma	Foma/*Vrs1.b3* (9)	Propyl Methane Sulfonate	Lundqvist 1991(10)	Mis-sense	Transition (C to T) 194bp
4	*int-e.26*	Foma	Foma/*Vrs1.b3* (9)	Neutrons + Ethyl Methane Sulfonate	Lundqvist 1991(10)	Non-sense	Transition (C to T)/490bp
5	BW-NIL(*int-e.58*)	Kristina	Bowman/*Vrs1.b3* (11)	Ethyl Methane Sulfonate	Lundqvist 1991(10) Druka et al 2011(4)	Mis-sense	Transition (C to T) 248bp
6	*int-e.65*	Bonus	Bonus/*Vrs1.b3* (9)	Sodium Azide	Lundqvist 1991(10)	Mis-sense	Transition (G to A)/68bp
7	*int-e.66*	Kristina	Kristina/*Vrs1.b3* (9)	Ethyl Methane Sulfonate	Lundqvist 1991(10)	Mis-sense	Transition (C to T)/428bp
8	*int-e.72*	Bonus	Bonus/*Vrs1.b3* (9)	X-rays	Unpublished	Mis-sense	Transition (C to T) 248bp
9	*int-e.87*	Bonus	Bonus/*Vrs1.b3* (9)	Sodium Azide	Unpublished	Mis-sense	Transition (G to A)/74bp
10	*int-e.89*	Hege	Hege/*Vrs1.b*	Sodium Azide	Unpublished	Mis-sense	Transition (G to A)/68bp
11	*int-e.90*	Hege	Hege/*Vrs1.b*	Sodium Azide	Unpublished	Mis-sense	Transition (G to A)/68bp
12	*int-e.91*	Hege	Hege/*Vrs1.b*	Sodium Azide	Unpublished	Mis-sense	Transition (G to A)/68bp
13	*int-e.92*	Hege	Hege/*Vrs1.b*	Sodium Azide	Unpublished	Mis-sense	Transition (G to A)/68bp
14	*int-e.101*	Hege	Hege/*Vrs1.b*	Sodium Azide	Unpublished	Mis-sense	Transition (G to A)/74bp
15	*int-e.128*	Foma	Foma/*Vrs1.b3* (9)	X-rays	Unpublished	Non-sense	Transition (A to G)/1bp
16	BW-NIL(*vrs4.k*)	MFB104	Bowman/*Vrs1.b3* (11)	Gamma rays	Fukuyama *et al.*(12); Druka *et al.*2011(4)	Non-sense	Deletion (1bp)/72-72bp
17	BW-NIL (*mul1.a*)	Montcalm	Bowman/*Vrs1.b3* (11)	Gamma rays	Kasha & Walker (13); Druka *et al.*2011(4)	Non-sense	Deletion (11bp)/44-54bp
18	*vrs4.l* (*syn. Xc 41.5*)	Piroline	Piroline/*Vrs1.b*	X-rays	Fukuyama *et al.* (12)	Non-sense	Deletion (14bp)/528-546bp
19	MHOR318	Ackermann's Donaria	Ackermann's Donaria/*Vrs1.b*	X-rays	Unpublished	Gene deletion	—
20	MHOR345	Heine's Haisa	Heine's Haisa /*Vrs1.b3* (14)	X-rays	Unpublished	Gene deletion	—

*Nucleotide positions of lesions in different *vrs4* mutant alleles with respect to reference sequence of *HvRA2*. See Fig. S5 for *HvRA2* reference sequence (GenBank accession KC854554) and mutations in different *vrs4* alleles mapped to the ORF.

**Reference stating the allelic status at *Vrs1* locus.

Table S5. BAC clones sequenced in *Vrs4* gene region on 3HS

BAC Clone #	BAC Clone name	BAC length (Kb)
1	HVVMRXALLeA0166J14	81
2	HVVMRXALLmA0525L04	155
3	HVVMRXALLrA0402J12	157
4	HVVMRXALLmA0524F02	116
5	HVVMRX83khA0179C14	94
6	HVVMRXALLhC0084K10	69
7	HVVMRXALLrA0075M21	49
8	HVVMRXALhLB0083N17	83
9	HVVMRX83KhA0016A06	69
10	HVVMRXALhLB0066O05	100
11	HVVMRXALLrA0390E03	120
12	HVVMRXALLeA0100K09	145
13	HVVMRXALLeA0170A17	98
14	HVVMRXALLmA0292B07	138
15	HVVMRXALLeA0349L07	111
16	HVVMRXALLeA0332L11	95
17	HVVMRXALLeA0217N06	138
18	HVVMRXALLmA0279J11	122
19	HVVMRXALLmA0260B08	105
20	HVVMRXALLmA0383N08	95
21	HVVMRXALLeA0271J13	111
22	HVVMRXALLeA0253H10	88

Table S6. Monocot RAMOSA2 orthologs, RAMOSA2-LIKE sequences from eudicots and LBD proteins used for phylogenetic analysis.

#	Annotation	Query cover (%)	E-value	Max identity (%)	Accession/ Morex contig	Phylogenetic clade
1	RAMOSA2 [*Hordeum vulgare*]	100	0.0	100	ABC54561.1	RAMOSA2 ortholog/homolog
2	RAMOSA2 [*Triticum durum*]	100	5E-165	93	ADJ67794.1	RAMOSA2 ortholog/homolog
3	RAMOSA2 [*Aegilops tauschii*]	100	2E-169	95	EMT25999.1	RAMOSA2 ortholog/homolog
4	RAMOSA2 [*Oryza sativa Japonica* Group]	93	2E-125	79	ABU44495.1	RAMOSA2 ortholog/homolog
5	RAMOSA2 [*Loudetia sp.* MCE-2012]	94	2E-122	79	AFJ42326.1	RAMOSA2 ortholog/homolog
6	RAMOSA2 [*Chrysopogon gryllus*]	93	6E-112	72	AFJ42327.1	RAMOSA2 ortholog/homolog
7	RAMOSA2 [*Triticum aestivum*]	100	3E-158	94	ABK79907.1	RAMOSA2 ortholog/homolog
8	RAMOSA2 [*Schizachyrium sanguineum var. hirtiflorum*]	93	2E-101	69	AFJ42332.1	RAMOSA2 ortholog/homolog
9	RAMOSA2 [*Sorghum bicolor*]	94	3E-104	69	AFJ42334.1	RAMOSA2 ortholog/homolog
10	RAMOSA2 [*Andropogon hallii*]	94	1E-99	69	AFJ42331.1	RAMOSA2 ortholog/homolog
11	RAMOSA2 [*Zea mays*]	100	2E-112	73	NP_001131918.1	RAMOSA2 ortholog/homolog
12	RAMOSA2 [*Phacelurus digitatus*]	100	1E-110	73	AFJ42333.1	RAMOSA2 ortholog/homolog
13	RAMOSA2 [*Andropterum stolzii*]	94	8E-103	70	AFJ42330.1	RAMOSA2 ortholog/homolog
14	RAMOSA2 [*Brachypodium distachyon*]	100	5E-117	77	XP_003569245.1	RAMOSA2 ortholog/homolog
15	RAMOSA2 [*Brachypodium sylvaticum*]	100	1E-108	75	CCF55439.1	RAMOSA2 ortholog/homolog
16	RAMOSA2 [*Cymbopogon flexuosus*]	100	2E-101	67	AFJ42328.1	RAMOSA2 ortholog/homolog
17	ELONGATED PETIOULE1 (ELP1) - [*Glycine max*]	48	2E-67	77	AFK81066.1	RAMOSA2 ortholog/homolog
18	LBD PROTEIN-LIKE [*Glycine max*]	48	3E-67	77	XP_003527004.1	RAMOSA2 ortholog/homolog
19	ELONGATED PETIOULE2 - [*Glycine max*]	48	7E-67	75	XP_003523096.1	RAMOSA2 ortholog/homolog
20	LBD PROTEIN-LIKE [*Cicer arietinum*]	45	5E-67	81	XP_004515877.1	RAMOSA2 ortholog/homolog
21	LBD PROTEIN-LIKE [*Glycine max*]	49	5E-66	77	ACU23406.1	RAMOSA2 ortholog/homolog
22	SLEEPLESS (SLP) - ortholog of ELP1 - [*Lotus japonicus*]	63	5E-68	63	AFK81064.1	RAMOSA2 ortholog/homolog
23	ELONGATED PETIOULE1 (ELP1) - [*Medicago truncatula*]	45	4E-66	79	AFK81063.1	RAMOSA2 ortholog/homolog
24	LBD PROTEIN-LIKE [*Cicer arietinum*]	45	4E-64	78	XP_004501886.1	RAMOSA2 ortholog/homolog
25	APULVINIC (APU) - ortholog of ELP1 - [*Pisum sativum*]	45	4E-65	78	AFK81065.1	RAMOSA2 ortholog/homolog
26	LBD PROTEIN-LIKE [*Cucumis sativus*]	45	2E-67	81	XP_004173060.1	RAMOSA2 ortholog/homolog
27	LBD PROTEIN-LIKE [*Ricinus communis*]	51	9E-69	78	XP_002511341.1	RAMOSA2 ortholog/homolog
28	LBD PROTEIN-LIKE [*Populus trichocarpa*]	48	1E-68	81	XP_002318660.1	RAMOSA2 ortholog/homolog
29	LBD PROTEIN-LIKE [*Theobroma cacao*]	48	2E-68	81	EOY20851.1	RAMOSA2 ortholog/homolog
30	LBD PROTEIN-LIKE [*Prunus persica*]	47	3E-67	79	EMJ12162.1	RAMOSA2 ortholog/homolog
31	LBD PROTEIN-LIKE [*Fragaria vesca subsp. vesca*]	50	1E-67	75	XP_004298984.1	RAMOSA2 ortholog/homolog
32	LBD PROTEIN-LIKE [*Solanum lycopersicum*]	49	1E-66	77	XP_004236250.1	RAMOSA2 ortholog/homolog
33	LBD PROTEIN-LIKE [*Capsella rubella*]	57	3E-63	67	EOA15040.1	RAMOSA2 ortholog/homolog
34	ASSYMETRIC LEAVES2-LIKE4 (ASL4) [*Arabidopsis thaliana*]	43	4E-63	81	NP_201114.1	RAMOSA2 ortholog/homolog
35	LBD PROTEIN-LIKE [*Solanum lycopersicum*]	45	2E-61	74	XP_004242158.1	RAMOSA2 ortholog/homolog
36	LBD PROTEIN-LIKE [*Vitis vinifera*]	46	2E-68	82	XP_002281358.1	RAMOSA2 ortholog/homolog
37	LBD PROTEIN25-LIKE [*Cucumis sativus*]	45	2E-64	79	XP_004169034.1	RAMOSA2 ortholog/homolog
38	LBD PROTEIN25-LIKE [*Cucumis sativus*]	49	5E-63	75	XP_004156730.1	RAMOSA2 ortholog/homolog

39	LBD PROTEIN-LIKE [*Arabidopsis thaliana*]	45	2E-57	74	BAB02689.1	RAMOSA2 ortholog/homolog
40	LBD PROTEIN-LIKE [*Vitis vinifera*]	45	3E-63	76	XP_002273053.1	RAMOSA2 ortholog/homolog
41	LBD PROTEIN-LIKE [*Theobroma cacao*]	45	2E-66	79	EOY02489.1	RAMOSA2 ortholog/homolog
42	LBD PROTEIN-LIKE [*Prunus persica*]	45	6E-63	80	EMJ18120.1	RAMOSA2 ortholog/homolog
43	LBD PROTEIN-LIKE [*Ricinus communis*]	46	1E-64	78	XP_002521459.1	RAMOSA2 ortholog/homolog
44	LBD PROTEIN-LIKE [*Populus trichocarpa*]	45	2E-65	79	XP_002300051.1	RAMOSA2 ortholog/homolog
45	LBD PROTEIN25-LIKE [*Glycine max*]	46	1E-62	75	XP_003554815.1	RAMOSA2 ortholog/homolog
46	LBD PROTEIN25-LIKE [*Glycine max*]	45	2E-65	79	XP_003548568.1	RAMOSA2 ortholog/homolog
47	LBD PROTEIN25 [*Glycine max*]	45	6E-65	78	XP_003553820.1	RAMOSA2 ortholog/homolog
48	LBD PROTEIN-LIKE [*Cucumis sativus*]	47	5E-61	74	XP_004157828.1	RAMOSA2 ortholog/homolog
49	LBD PROTEIN-LIKE [*Prunus persica*]	45	7E-48	66	EMJ13351.1	LBD protein (CLASS I)
50	LBD PROTEIN4-LIKE [*Fragaria vesca subsp. vesca*]	45	4E-49	66	XP_004293726.1	LBD protein (CLASS I)
51	LBD PROTEIN-LIKE [*Populus trichocarpa*]	45	2E-47	65	XP_002304584.1	LBD protein (CLASS I)
52	LBD PROTEIN4 isoform 1 [*Theobroma cacao*]	45	2E-48	66	EOY27472.1	LBD protein (CLASS I)
53	LBD PROTEIN4 [*Vitis vinifera*]	45	8E-48	64	XP_002270650.1	LBD protein (CLASS I)
54	LBD PROTEIN4-LIKE [*Cicer arietinum*]	45	2E-47	64	XP_004505337.1	LBD protein (CLASS I)
55	LBD PROTEIN-LIKE - LOC100790989 [*Glycine max*]	47	6E-48	60	NP_001241363.1	LBD protein (CLASS I)
56	LBD PROTEIN4-LIKE [*Solanum lycopersicum*]	45	1E-48	65	XP_004250781.1	LBD protein (CLASS I)
57	LBD PROTEIN-LIKE [*Ricinus communis*]	50	3E-50	60	XP_002513395.1	LBD protein (CLASS I)
58	LBD PROTEIN4 [*Theobroma cacao*]	46	2E-48	64	EOY13865.1	LBD protein (CLASS I)
59	LBD PROTEIN-LIKE [*Medicago truncatula*]	45	3E-47	64	XP_003616690.1	LBD protein (CLASS I)
60	LBD PROTEIN-LIKE [*Theobroma cacao*]	47	3E-49	63	EOY34594.1	LBD protein (CLASS I)
61	LBD PROTEIN-LIKE [*Vitis vinifera*]	47	4E-48	64	CAN68873.1	LBD protein (CLASS I)
62	LBD PROTEIN-LIKE [*Prunus persica*]	47	4E-48	64	EMJ07197.1	LBD protein (CLASS I)
63	LBD PROTEIN6-like [*Cucumis sativus*]	50	8E-55	65	XP_004152887.1	LBD protein (CLASS I)
64	LBD PROTEIN6-like [*Glycine max*]	61	6E-48	57	XP_003545810.1	LBD protein (CLASS I)
65	LBD PROTEIN-LIKE [*Capsella rubella*]	51	3E-47	64	EOA35742.1	LBD protein (CLASS I)
66	LBD PROTEIN-LIKE [*Populus trichocarpa*]	59	5E-49	58	XP_002307250.1	LBD protein (CLASS I)
67	LBD PROTEIN36-like [*Cucumis sativus*]	51	1E-47	62	XP_004148465.1	LBD protein (CLASS I)
68	LBD PROTEIN-LIKE [*Prunus persica*]	53	1E-47	61	EMJ04878.1	LBD protein (CLASS I)
69	LBD PROTEIN1-LIKE *[Hordeum vulgare*]	—	8E-57	—	Ctg135924_5HL	LBD protein (CLASS I)
70	LBD PROTEIN15-LIKE [*Hordeum vulgare*]	—	3E-23	—	Ctg1572307_3HL	LBD protein (CLASS I)
71	LBD PROTEIN1-LIKE [*Hordeum vulgare*]	—	9E-18	—	Ctg62778_4HL	LBD protein (CLASS I)
72	LBD PROTEIN11-LIKE [*Hordeum vulgare*]	—	2E-52	—	Ctg54974_1H	LBD protein (CLASS I)
73	LBD PROTEIN18-LIKE [*Hordeum vulgare*]	—	9E-12	—	Ctg1591863_7HS	LBD protein (CLASS I)
74	LBD PROTEIN16-LIKE [*Hordeum vulgare*]	—	2E-27	—	Ctg46032_6HL	LBD protein (CLASS I)
75	LBD PROTEIN24-LIKE [*Hordeum vulgare*]	—	9E-18	—	Ctg47723_4HL	LBD protein (CLASS I)
76	LBD PROTEIN6-LIKE [*Hordeum vulgare*]	—	2E-76	—	Ctg61827_3HL	LBD protein (CLASS I)
77	LBD PROTEIN6-LIKE [*Hordeum vulgare*]	—	3E-81	—	Ctg45166_1H	LBD protein (CLASS I)
78	LBD PROTEIN6-LIKE [*Hordeum vulgare*]	—	2E-76	—	Ctg51474_4HS	LBD protein (CLASS I)
79	LBD PROTEIN7-LIKE [*Hordeum vulgare*]	—	4E-09	—	Ctg98873_3HL	LBD protein (CLASS I)
80	LBD PROTEIN-LIKE [*Hordeum vulgare*]	—	4E-10	—	Ctg38897_5HL	LBD protein (CLASS I)

81	LBD PROTEIN41-LIKE; Class II [*Hordeum vulgare*]	—		—	Ctg42541_2HL	LBD protein (CLASS II)
82	LBD PROTEIN38-LIKE; Class II [*Hordeum vulgare*]	—		—	Ctg36895	LBD protein (CLASS II)
83	LBD PROTEIN39-LIKE; Class II [*Hordeum vulgare*]	—		—	Ctg1561909	LBD protein (CLASS II)
84	LBD PROTEIN41-LIKE; Class II [*Hordeum vulgare*]	—		—	Ctg50476_4HL	LBD protein (CLASS II)

References

1. Chen X, *et al.* (2005) Mutation of the *RESURRECTION1* locus of Arabidopsis reveals an association of cuticular wax with embryo development. *Plant Physiol.* 139(2):909-919.
2. Forster BP, *et al.* (2007) The barley phytomer. *Ann. Bot.* 100(4):725-733.
3. Fukuyama T, Takahashi R, & Hayashi J (1982) Genetic studies on the induced six-rowed mutants in barley. *Ber. Ohara Inst. landw. Biol., Okayama Univ.* 18:99-113.
4. Druka A, *et al.* (2011) Genetic dissection of barley morphology and development. *Plant Physiol.* 155(2):617-627.
5. Doyle JJ & Doyle JL (1990) Isolation of plant DNA from fresh tissue. *Focus* 12:13-15.
6. Komatsuda T, Nakamura I, Takaiwa F, & Oka S (1998) Development of STS markers closely linked to the vrs1 locus in barley, Hordeum vulgare. *Genome* 41(5):680-685.
7. Thompson JD, Higgins DG, & Gibson TJ (1994) CLUSTAL W: improving the sensitivity of progressive multiple sequence alignment through sequence weighting, position-specific gap penalties and weight matrix choice. *Nucleic Acids Res.* 22(22):4673-4680.
8. Shuai B, Reynaga-Pena CG, & Springer PS (2002) The *LATERAL ORGAN BOUNDARIES* gene defines a novel, plant-specific gene family. *Plant Physiol.* 129(2):747-761.
9. Komatsuda T, *et al.* (2007) Six-rowed barley originated from a mutation in a homeodomain-leucine zipper I-class homeobox gene. *Proc. Natl. Acad. Sci. USA* 104(4):1424-1429.
10. Lundqvist U (1991) Coordinator's report: Ear morphology genes. *Barley Genetics Newsletter* 20:85.
11. Cuesta-Marcos A, *et al.* (2010) Genome-wide SNPs and re-sequencing of growth habit and inflorescence genes in barley: implications for association mapping in germplasm arrays varying in size and structure. *BMC Genomics* 11:707.
12. Fukuyama T, Hayashi J, & Takahashi R (1975) Genetic and linkage studies of five types of induced six-row mutants. *Barley Genetics Newsletter* 5:12-13.
13. Kasha KJ & Walker GWR (1960) Several recent barley mutants and their linkages. *Can. J. Genet. Cytol.* 2:397-415.
14. Ramsay L, *et al.* (2011) *INTERMEDIUM-C*, a modifier of lateral spikelet fertility in barley, is an ortholog of the maize domestication gene *TEOSINTE BRANCHED1*. *Nat. Genet.* 43(2):169-172.